

# Analysis of hygrothermally induced fiber fracture in single fiber composite using fiber Bragg grating

M. Lai<sup>1</sup>, J. Cugnoni<sup>1</sup>, and J. Botsis<sup>1a</sup>

<sup>1</sup>Ecole Polytechnique Federale de Lausanne (EPFL)  
LMAF-IGM-STI, Station 9, Lausanne CH-1015, Switzerland

**Abstract.** Hygro-thermal ageing of composite materials introduces a modification in the material properties of its constituents and the development of stresses that can lead to severe local damage like fracture of the reinforcing fibers and de-bonding of the latter from the matrix. The study of the complex stress field generated by this induced damage is helpful in designing more resistant materials. Modelling strain-stress field in the vicinity of these discontinuities has led to the development of different analytical models like for instance shear lag models based on simplification assumptions. Recently the development of embedded optical sensors allowed to shed light on the assumptions made, since they can be used, at the same time, as reinforcement and sensors and thus being capable to give information on the strain distributions during the evolution of the damage. In this work a single fiber composite, whose reinforcement is an optical sensor, is used in order to investigate the complex strain field generated by the fiber fracture caused by the matrix swelling during water uptake.

## 1 Introduction

It is well known that the global response of composites materials is linked to the fiber matrix interface as well as to the fiber integrity. Many efforts have been devoted in the past in understanding the stress transfer between fiber and matrix and the adhesion energy of the components in order to improve the mechanical performance of the composite itself. With this aim numerous experimental techniques in particular, fiber fragmentation [1], fiber pull out and micro-debonding tests, as well as theoretical approaches including shear lag analysis [2] and its successive modifications have been developed. However, the relevant parameters determined using such experimental techniques are strongly dependent on fiber sizing, residual stresses present in the composite as well as hygro-thermal ageing to which the structure can be subjected during service life.

Another difficulty is to acquire experimental data regarding stress/strain fields inside the material close to the interface where debonding takes place or close to a fiber fracture. Such data have been obtained with Raman microscopy [3] but usually they are noisy. Information about the strain fields in these locations can be retrieved also by distributed sensing using long fiber Bragg grating (FBG) and optical low coherence reflectometry (OLCR) presenting much higher signal to noise ratio. Such data accompanied by pertinent stress analysis can lead to a better understanding of such phenomena. In this paper debonding and fiber fracture of the reinforcement are examined in the case of cylindrical single fiber composite having as reinforcement an optical fiber with FBG. Firstly residual strains due to processing induced shrinkage are analyzed, secondly, the evolution of mechanical properties of the pure matrix is investigated as function of water uptake, and thirdly, as a fiber fracture is produced due to the tensile load generated by the matrix's expansion, the strain on the fiber is retrieved and discussed in the light of the shear lag model.

---

<sup>a</sup> e-mail : john.botsis@epfl.ch

## 2 Materials

The epoxy under investigation is a mixture of two resins DER330<sup>®</sup> DER732<sup>®</sup> and the hardener DEH26<sup>®</sup> provided by the DOW chemical company. This mixture was stirred in vacuum in fixed weight proportion of 70:30:10, respectively, and casted in a vertical mould that keeps the optical fiber with the sensor axially aligned. The resulting specimen is a cylinder of 12mm in diameter and a length of 40mm (Fig. 1). In this configuration the fibre plays the role of reinforcement and sensor for distributed strains measurement along the fibre direction.

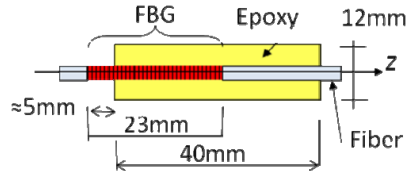


Fig. 1. Single fiber composite section

The single mode optical fibre with diameter of 125 $\mu$ m contains a fiber Bragg grating (FBG) 23mm long. More information about specimen preparation and thermal cycles are provided in [4] After processing, the specimens are placed in a bath at 50 $^{\circ}$ C containing demineralised water.

Control specimens with the same geometry and optical fibres, without FBG, were placed in the same environment and periodically weighted, using a digital balance with a resolution of 0.01mg, in order to retrieve the water uptake and construct the absorption curve for this configuration. In the same bath, 6 sets of 5 cylindrical dogbone-like specimens were aged and successively tested, at different water contents, in traction or subjected to relaxation tests into the water using a specially designed bath in order to keep the temperature controlled and to prevent moisture desorption from the specimens. Considering the low speed of diffusion compared to the testing time, additional absorption during the mechanical tests is considered insignificant.

## 3 Optical measurements of strains along the FBG

Residual and hygrothermal strains have been monitored using OLCR [5] and the layer peeling technique that allows for the local Bragg wavelength (LBW) reconstruction. Once the local wavelength is known, local strains can be calculated using:

$$\frac{\lambda_B(z) - \lambda_{B0}}{\lambda_{B0}} = (1 - p_e) \varepsilon_z(z) + (\alpha_f + \xi) \Delta T \quad (1)$$

where the  $z$  is the axial direction,  $p_e$  is a grating gage factor equal to 0.2148 [5],  $\lambda_{B0}$  is the reference Bragg wavelength,  $\lambda_B(z)$  is the local Bragg wavelength,  $\xi \approx 8.9 \times 10^{-6}$  [6] and  $\Delta T$  are the thermo-optic constant and temperature change respectively and  $\alpha_f \approx 8 \times 10^{-7} \text{ } ^{\circ}\text{C}^{-1}$  is the fiber coefficient of thermal expansion. Note that because of the difference in the order of magnitude between  $\alpha_f$  and  $\xi$  only the latter is considered in the second term of (1).

## 4 Residual stresses

Using as reference wavelength in (1) the wavelength recorded prior embedding and as local Bragg wavelength the one calculated after post curing, the residual axial strain distribution imposed to the fiber due to processing has been determined and it is reported in Fig. 2. The residual stress field is of great importance in micromechanics analysis, firstly because it represents the initial condition of the

sample and, and secondly because the correct evaluation of shear load transmitted to the fiber in case of debonding with friction depends on the radial component of the stress whose major part is built during processing. The capability of capturing the axial strain field demonstrated in Fig. 2 allows for the use of the crack compliance method in order to infer information on the radial distribution of the residual strain field in the specimen [7].

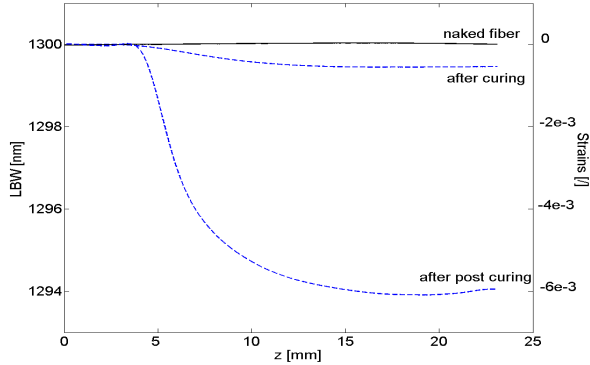


Fig. 2 Axial residual strains development during processing.

### 5 Absorption Curve

In order to determine the two parameters involved in the water diffusion kinetic trough the resin, i.e., diffusivity and saturation point, the reference and dog-bone like specimens were periodically weighted, at different intervals of time for an immersion period of approximately one year. The absorption curve from the dog-bone specimens is reported in Fig. 3 where water gain percentage  $w_g\%$  is defined as  $w_g\% = [(W(t) - W(0)) / W(0)] \cdot 100$  in which  $W$  are the weights of the specimen at 0 and  $t$  times, respectively.

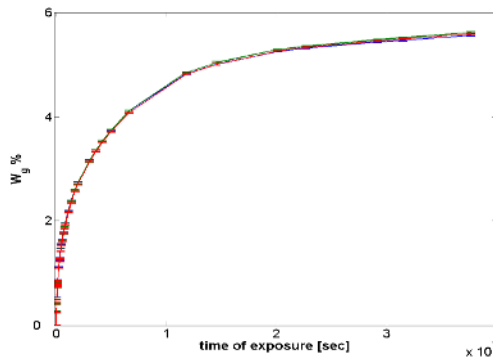


Fig. 3 Absorption curve for three reference specimens.

Using identification procedure it has been possible to determine the saturation point  $s \approx 5.7w_g\%$ , as the horizontal tangent at very long time, and the diffusivity which can be considered linear function of the concentration whose extreme values are  $D(c=0)=2.1453 \times 10^{-6} \text{ mm}^2/\text{s}$  and  $D(c=s)=2.7607 \times 10^{-7} \text{ mm}^2/\text{s}$ . In fact, a pure Fickian diffusive model was found poor in representing the experimental absorption curves in the short time and gave an underestimation of the absorption kinetic.

## 6 Mechanical Properties

In order to establish the influence of water uptake on the mechanical properties of the epoxy, tensile and relaxation tests were conducted on dog-bone specimens. Young's moduli and long term relaxation moduli have thus been determined in dry condition at 50°C, corresponding to the temperature of the ageing bath, and at 50°C at different percentage of moisture content. The tests in dry conditions were conducted in a climatic chamber with forced circulation of dry hot air, whereas tests with already aged samples were performed under water.

Since relatively high temperature plays an important role in lowering material properties particular attention was paid to perform tests after achieving thermal equilibrium with the testing environment. Short and long time moduli are summarized in Fig. 4.

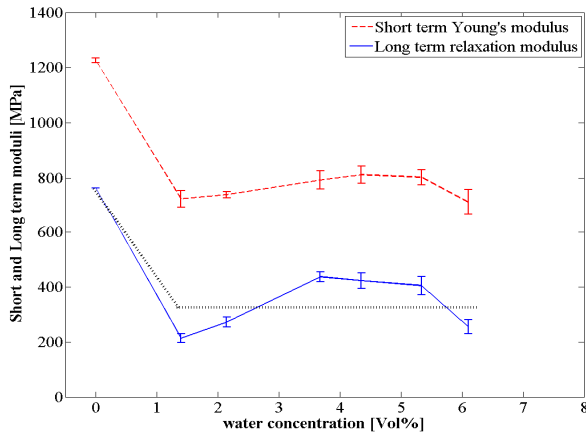


**Fig. 4** Short and long term moduli evolution against water uptake at 50°C and long modulus approximation (dotted line)

In addition, the determined characteristic relaxation times are much shorter than the diffusion phenomenon, thus justifying the assumption that only the long term relaxation modulus is important in determining the response of the material. In the following, the behaviour introduced by the water content on the long term modulus also simplified by considering a plateau in the zone at concentrations greater than 1Vol% (Fig. 4 dotted straight line).

## 7 Coefficient of moisture expansion

Once the single fiber composite is immersed into the ageing bath at 50°C, it expands due to the raise of temperature and it starts to swell progressively because of the increasing volume of water retained by the matrix. After the thermal equilibrium has been achieved, all the successive volume modifications are induced by deformation of the matrix due to the water absorption. The relationship that expresses the hygroscopic strains  $\varepsilon^h$  as function of the concentration is the following:

$$\varepsilon^h = \beta(\bar{c})\bar{c}(t) \quad (2)$$

where  $\bar{c}(t)$  is the average water content expressed in volume fraction using  $\bar{c}(t) = (\rho_e / \rho_w) w_g \%$  in

which  $\rho_e = 1.2 \text{ g/cm}^3$  and  $\rho_w = 1 \text{ g/cm}^3$  are the densities of epoxy and water, respectively;  $\beta(\bar{c})$  is the

coefficient of moisture expansion (CME), usually is considered independent of the concentration and that, as will be shown later, it can be considered so only as a first approximation.

The presence of the FBG inside the specimen provides a unique tool to measure the axial deformation to which the fiber is subjected due to the water absorption. Using Eq. (1) the evolution of strains as function of time is calculated and reported in Fig. 5 where it is possible to notice essentially three zones. In the first one the sensor is outside of the specimen and is subjected only to thermal strains, in the second zone a non homogeneous strain field is felt due to the presence of the edge of the specimen, whereas in the inner zone a plateau is reached. In this zone the strain field is assumed uni-dimensional and after thermal equilibrium, the axial deformation can be approximated by (2).

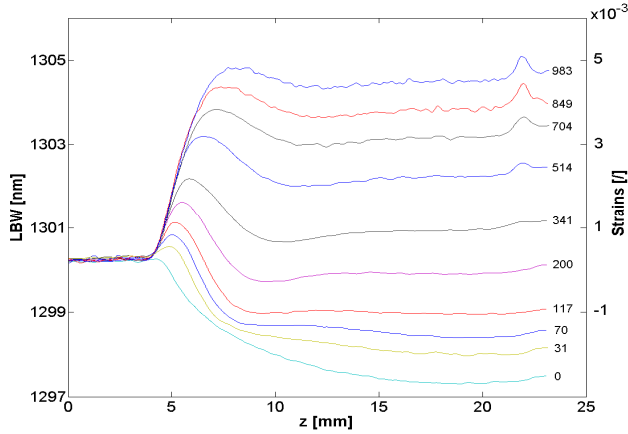


Fig. 5 Evolution of fiber strains during ageing.

Using the  $\bar{c}(t)$  measurements, the values of incremental hygric strains obtained from the data in Fig. 5 and (1) at  $z = 20\text{mm}$  where no side effects are present, are plotted in Fig. 6 against water concentration.

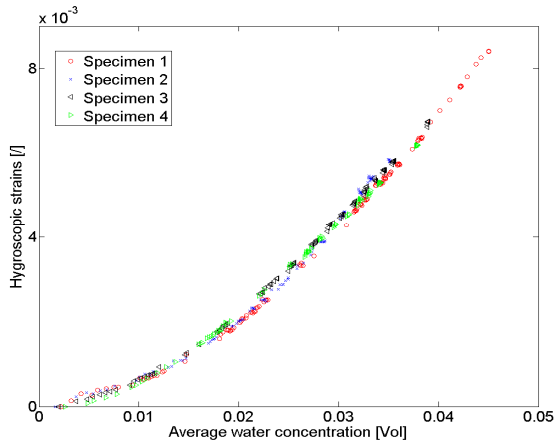


Fig. 6 Hygroscopic strains evolution against concentration.

By definition the slope of the curve represents the coefficient of moisture expansion. Note that  $\beta$  is not constant and for small values of water concentration it presents a strong non linearity.

## 8 Fiber fracture

As anticipated, due to the high tensile deformation imposed by the matrix expansion, fiber fracture occurred inside the FBG allowing the investigation of the stress field generated by this discontinuity. The development of fiber strains, as function of absorption time, around a fiber fracture located at  $z \approx 16\text{mm}$  is reported in Fig. 7.

The first shear lag model was proposed by Cox in 1952 [2] under the assumption that the shear force, developed because of the simultaneous presence of matrix and reinforcement during external loading, is proportional to the difference of displacement of the two constituents. For linear elastic materials and an intact interface the axial strain evolution along the fiber can be represented, for a long fiber, as follows [8]:

$$\varepsilon_z^f(z) = \varepsilon_{z,\infty}^f [1 - \exp(-\gamma z)] \quad (3)$$

where  $\varepsilon_{z,\infty}^f$  represents far field strains on the fiber and  $\gamma$  is a parameter function of the material properties and the geometry. With the axial strains distribution along the fiber determined using the FBG measurements it is thus possible to verify if, even in the case under investigation, the distribution (3) is representative of the strain field close to a fiber fracture and secondly allows the determination of the parameter  $\gamma$ . The experimental strains reported in Fig. 7 on the right side of the fracture have been approximated based on (3) and Cox's model is found to be indeed effective in depicting the recorded experimental behavior.

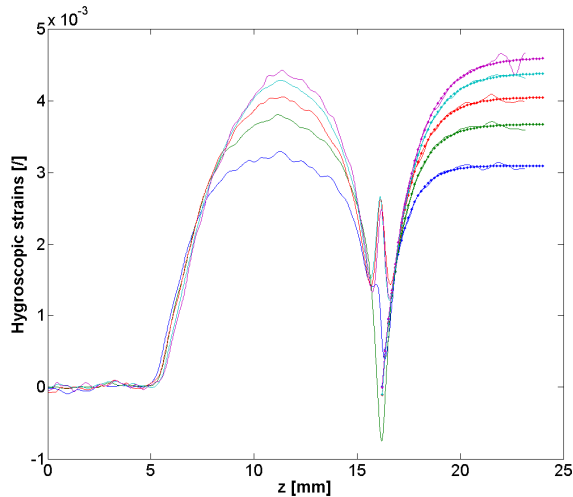


**Fig. 7** Experimental and calculated strains using Shear lag model in long fiber approximation.

Interestingly relation (3) describes the strain data very well with  $\gamma$  decreasing with time. This behaviour will be elucidated in another report. On the other hand, fiber matrix debonding with the presence of friction between surfaces can also be detected (Fig. 8) in the immediate left side of the fracture. Notice also that the extension of this zone increases with increasing ageing time.

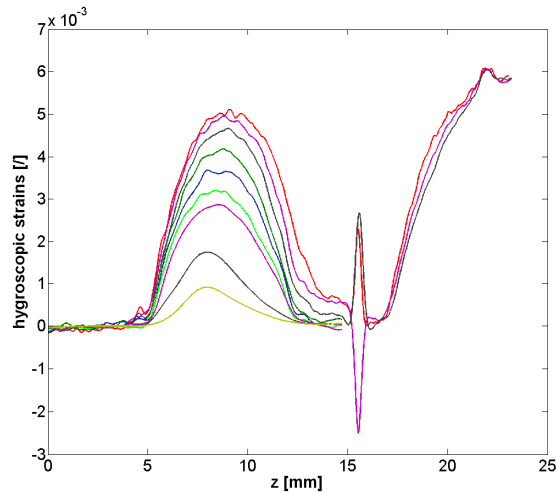


**Fig. 8** Experimental strains showing debonding with friction in the immediate left side of the fiber fracture

## 9 Conclusions and future works

Micromechanical analysis of composite materials during ageing should always be accompanied by the analysis of residual stress induced during processing and by a thorough understanding of the effect of water on the mechanical properties of its constituents. In addition, distributed strains measurement along the fiber has confirmed its great advantages in micromechanical analysis giving the unique possibility of investigating fiber fracture and debonding effects on the strain field developed during ageing. This precious data, especially if used in combination with appropriate finite element modelling can lead to the understanding of the interface deterioration in aggressive environments.

## Acknowledgments

The authors wish to acknowledge the financial support form the Swiss national science foundation under Grant 200020\_124397.

## References

1. Feillard P, Désarmot G, Favre JP. *A critical assessment of the fragmentation test for glass/epoxy systems*. Composites Science and Technology.;49(2):109-119,(1993).
2. Cox HL. *The elasticity and strength of paper and other fibrous materials*. British Journal of Applied Physics. (3):72, (1952).
3. Cervenka AJ, Bannister DJ, Young RJ. *Moisture absorption and interfacial failure in aramid/epoxy composites*. Composites Part A: Applied Science and Manufacturing; 29(9-10):1137-1144 (1998).
4. Lai M., Botsis J., Coric D., Cugnioni J. *On the degree of conversion and coefficient of thermal expansion of a single fiber composite using a FBG sensor*. In: Acierno D, Damore A, Grassia L, editors. 4th International Conference on Times of Polymers TOP and Composites, Ischia, ITALY: Amer Inst Physics; p. 135-137, (2008).
5. Giaccari P., Dunkel G. R., Humbert L., Botsis J., Limberger H. G., R.P. S. *On a direct determination of non-uniform internal strain fields using fibre Bragg gratings*. Smart Materials and Structures. (14):127, (2005).

6. Takahashi S, Shibata S. *Thermal variation of attenuation for optical fibers*. Journal of Non-Crystalline Solids;30(3):359-370, (1979).
7. Colpo F, Humbert L, Botsis J. *Characterisation of residual stresses in a single fibre composite with FBG sensor*. Composites Science and Technology; 67(9):1830-1841,(2007).
8. Daniel M.Isaac, Ori I., *Engineering Mechanics of Composite Materials*, Oxford, (2006).